Statistical analysis of flow field patterns in critical transition of a finite cylinder using an adaptive threshold method

Yu-Hsiang Chen[1*], Jiun-Jih Miau[1], Yng-Ru Chen[1]
1: Dept. of Aeronautics and Astronautics, National Cheng Kung University, Tainan, Taiwan 70101

* Correspondent author: pt8643631@gmail.com

Abstract
This study explores the intricate dynamics of flow around a finite circular cylinder of the aspect ratio 4 in the critical transition range with an adaptive threshold method. The analysis is focused on the formation of laminar separation bubbles (LSB), which is a key indicator of flow unsteadiness. Utilizing wind tunnel experiments, pressure signals were collected from different heights and angular positions on the cylinder. These signals were then compared with oil film visualization to define the presence of LSB using adaptive thresholds with a binary ranking technique. The results show that as the Reynolds number increased, the stability on the occurrence of separation bubbles is increased, particularly in the mid and upper sections of the cylinder. This new methodology offers a more comprehensive understanding of the complex, non-stationary flow behavior in the critical transition range, addressing the gaps left by the conventional analysis techniques.

Keyword: *Critical transition, Laminar separation bubbles, cylinder flow, Binary ranking method.*

1. Introduction

The flow field around a two-dimensional circular cylinder is a classic research topic in fluid mechanics, particularly in the critical transition range of laminar-turbulent flow. Roshko [1] elucidated the concept of separation bubbles formed in the critical transition range due to the boundary-layer transition. Achenbach[2] further elaborated that the critical transition range could be divided into the subcritical, critical, and supercritical ranges. Zdravkovich [3] summarized the research findings and defined the Reynolds number ranges corresponding to the regimes of pre-critical, single separation bubble, double separation bubble and supercritical. Miau at al. [4] made a detailed discussion on the three-dimensional characteristics of separation bubbles based on the results of oil-flow visualization.

Significant amount of studies have been made on finite circular cylinders with research interests in the complex flow characteristics in conjunction with the downwash motion from the free end with the formation of tip vortex and the horseshoe vortices in the base region with an upwash flow induced. [5] Okamoto and Sunabashiri [6] pointed out that the height-to-width ratio of 4 is a critical value, below which vortex shedding is a symmetric arch type, in contradictory to the Kármán type vortex shedding for the ratio above 4.

Flow in the critical transition range exhibits significant instability, asymmetry, and non-periodic variations. To study the flow characteristics in detail, Deshpande at al. [7] proposed a method ranking the state of flow around a sphere based on the PDFs of the real-time drag force signals to divide the critical transition range into sub-intervals, and determined a threshold value for each. By combining this with a binary method, the status concerned with the presence of separation bubble at each of the pressure taps measured on the cylinder was determined. Subsequently, a comprehensive diagram concerning the distribution of LSB on the sphere model was constructed, allowing for a description on the evolution of the states of separation bubble formation with Reynolds number in the critical transition range.

In this work, pressure measurements were made at various heights and angular positions on a finite-height circular cylinder in the critical transition range. The real-time pressure signals were collected and compared with the previous oil film visualization results. By combining a skewness analysis on the real-time signal traces and the concept of probability density function, we defined a threshold value to discriminate a condition whether laminar separation bubble named LSB is formed or not. Using this method, we statistically analyzed the occurrence frequency of LSB at each pressure tap. By collecting the information at 12 pressure taps on the model in a binary format over the time measured, the popularity of the states can be ranked in order. This method is aimed to establish a method to quantitatively describe the evolution of flow through in the critical transition region, in terms of the states in the binary format.

2. Methodology

2.1. Cylinder model

A finite-height circular cylinder was made of acrylic, with a diameter (D) of 150 mm and a height of 600mm. The pressure taps were located at three height levels on the cylinder: upper layer (z/D=3.5), middle layer (z/D=2), and lower layer (z/D=1). These taps were positioned at polar angles of θ= 0, ±70°, ±90°, ±110°, and 180°. A schematic of the experimental model and the coordinate system employed are given in Fig. 1.

In this study, the pressure coefficient (C_p) reduced from pressure measurement at a pressure tap is defined as $\frac{P}{\frac{1}{2}\rho U^2}$, where P denotes the dynamic pressure. The Reynolds number (Re) = $\frac{UD}{\nu}$, where U denotes the free stream velocity measured by a Pitot tube situated at the inlet of the test section and ν denotes the kinematic viscosity.

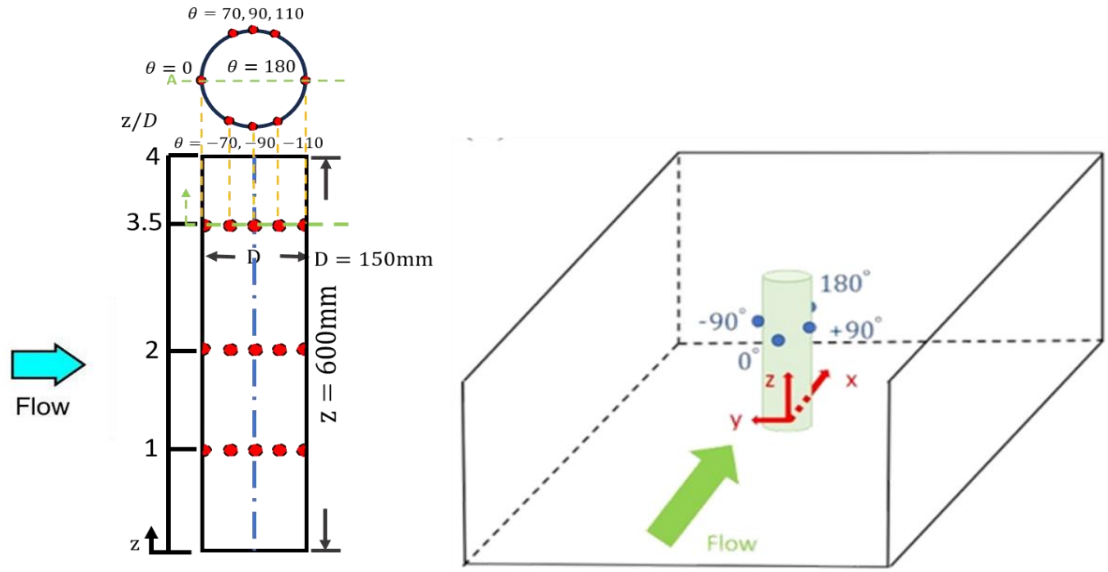

Fig. 1 Schematics of the experimental model and the coordinate system employed.

2.2. Wind tunnel

The wind tunnel for experiment is a low-speed open-circuit wind tunnel with a test section of 1 m by 1 m in cross section. The free stream velocity in the test section is ranged between 10 m/s and 40 m/s, for which the turbulence intensity is ranged between 0.55% and 0.7%. The blockage ratio of the cylinder model placed in this test section is 9%. The boundary layer thickness is 60 mm (0.4D) at a wind speed of 23.5 m/s and 56 mm (0.37D) at a wind speed of 31.9 m/s.

2.3. Adaptive threshold method

An adaptive threshold method was employed to determine a threshold value of C_p named C_{p2} to differentiate the status whether LSB is formed or not at the pressure tap measured. It involves three main steps.

Step 1: Establishing the Reference Threshold Value

The initial step is to determine a baseline value for the threshold concerning the LSB formation in the pre-critical regime. Following Lai et al. [8], the value is set to be -1.6 for C_p at the pressure taps at $\theta = \pm 90^o$ pressure taps. In addition, the value is set -1.4 for the pressure taps at θ=±110° based on our observations on the real-time pressure signals.

Step 2: Conducting a Skewness Analysis

The next step involves performing a skewness analysis on the pressure signals to classify the critical transition range into three flow regimes as indicated in Figs. 2a and b; 1: the pre-critical regime, 2: the one-bubble regime, and 3: the two-bubble regime.

Step 3: Calculating the Probability Density Function (PDF)

In the final step, the probability density function (PDF) of the C_p trace obtained at each of the pressure taps was examined. In a PDF distribution, the portion above the baseline threshold value defined for the pre-critical regime was excluded. Then, a local maximum in the remaining C_p distribution, named LC_{pmax}, was identified, which is indicated in a circle in Fig 2c. This value served as a reference to define a threshold value with regard to the experimental condition studied. This threshold value is named C_{p2}. It is indicated in Fig. 2c at the intersection of the red and green lines, whose PDF value is half of that of LC_{pmax} and $C_{p2} > LC_{pmax}$. In Fig. 2b a table lists the C_{p2} values determined for the three regimes at the pressure taps studied.

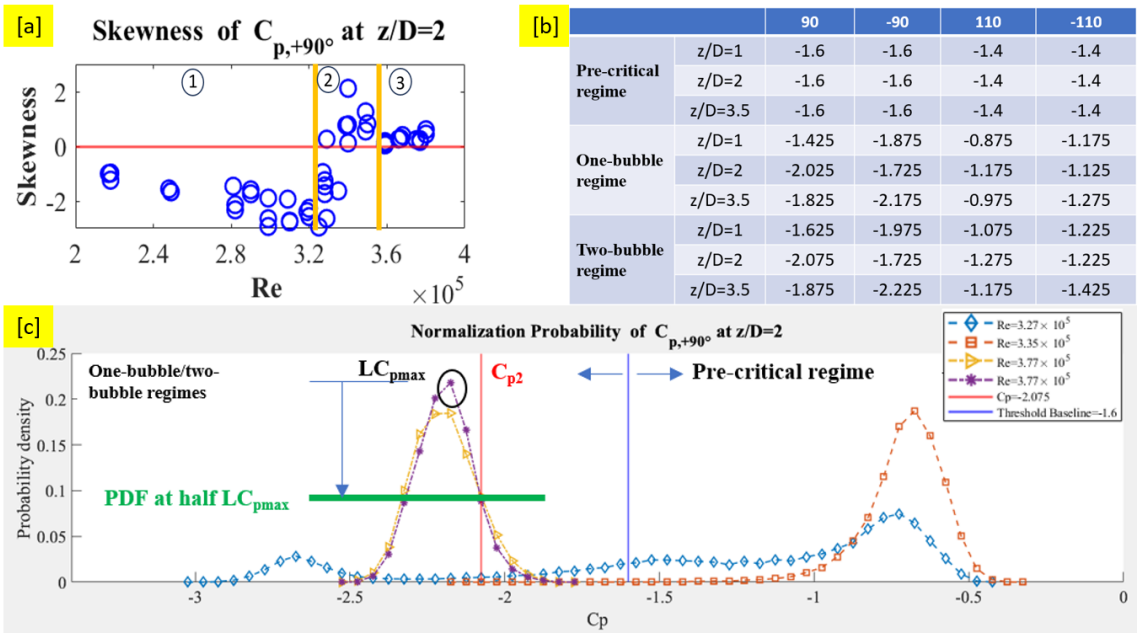

		90	-90	110	-110
Pre-critical regime	z/D=1	-1.6	-1.6	-1.4	-1.4
	z/D=2	-1.6	-1.6	-1.4	-1.4
	z/D=3.5	-1.6	-1.6	-1.4	-1.4
One-bubble regime	z/D=1	-1.425	-1.875	-0.875	-1.175
	z/D=2	-2.025	-1.725	-1.175	-1.125
	z/D=3.5	-1.825	-2.175	-0.975	-1.275
Two-bubble regime	z/D=1	-1.625	-1.975	-1.075	-1.225
	z/D=2	-2.075	-1.725	-1.275	-1.225
	z/D=3.5	-1.875	-2.225	-1.175	-1.425

Fig. 2 (a) A skewness distribution of C_p for illustration; 1: the pre-critical regime, 2: the one-bubble regime, and 3: the two-bubble regime. (b) A table listing the adaptive threshold values for different flow regimes and the pressure taps studied. (c) An illustration of the threshold value C_{p2} determined from a PDF distribution.

2.4. Binary ranking method

To determine the instantaneous status of LSB at a pressure tap measured, the C_p trace was examined by the adaptive threshold method described above. If C_p higher than C_{p2}, it is named a state without an LSB, marked by '0', otherwise it is named a state with an LSB, marked by '1'. Since the pressure measurements were made simultaneously at $\theta = \pm 90^o$ and $\pm 110^o$, z/D=1, 2 and 3.5, the status of bubble formation at the 12 locations at a time instant can be arranged as a 12 binary number, representing 2^{12} possible flow field configurations. The sequence of the binary numbers is defined in Fig 3a, and can be converted to a decimal format for easy interpretation. As a result, the popularity of each of the states can be ranked. An example is shown in Fig. 3b, which provides a distribution of the percentage values concerned with the top three states ranked at Re=3.2x10^5.

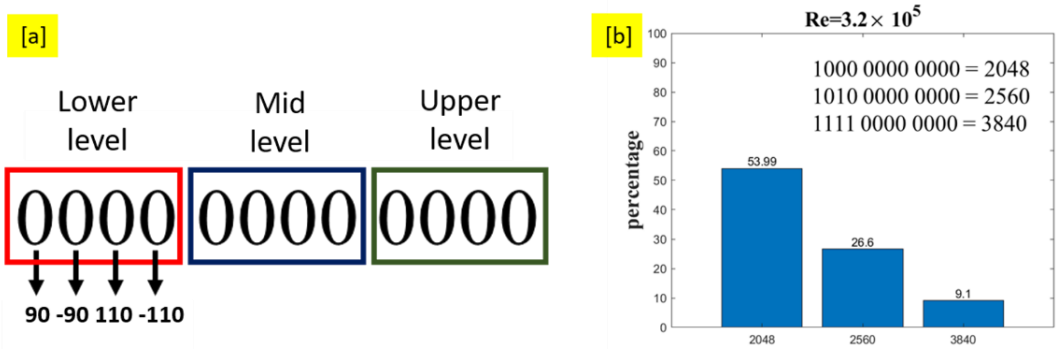

Fig. 3 (a) The LSB marks of each pressure hole are sorted by different heights and angles (b) The sorted columns are converted to decimal display.

3. Result and discussion

3.1 Verification of Adaptive Threshold and Binary ranking Methods

The adaptive threshold method described above is well-suited for analyzing the real-time pressure signals measured, which are characterized by pronouncedly non-stationary fluctuations due to unsteady formation of LSB. Its robustness in capturing the events of LSB formation can be illustrated in Fig. 4 with the C_p traces Re=3.4x10^5 shown. In Figs. 4a and 4b, it can be seen that even at θ= ±110^o, z/D=1 and 2, the fluctuations in the C_p traces are comparatively small in amplitude, this method can differentiate the states between LSB and non-LSB satisfactorily.

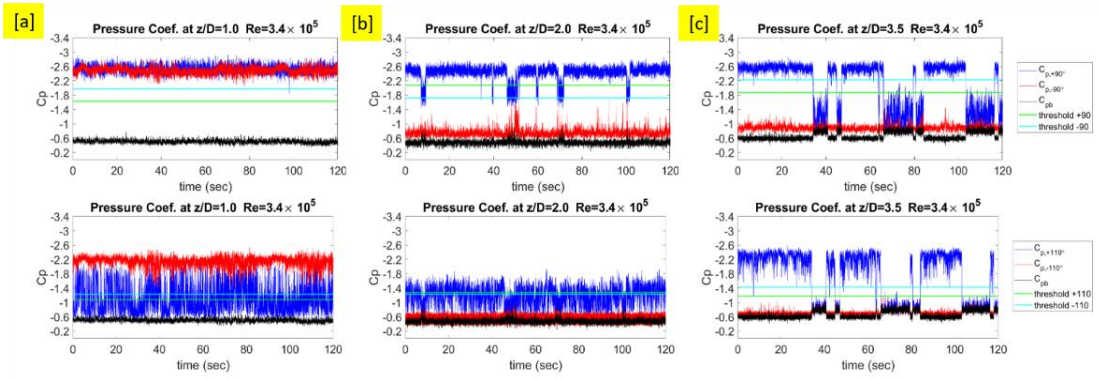

Fig. 4 The Cp traces at Re=3.4x10^5 with the threshold values indicated to validate the adaptive threshold method developed in this study.

3.2 Analysing critical region flow fields using adaptive thresholds and binary ranking methods

This method will be demonstrated with three scenarios. Starting with the flow in the pre-critical regime, a large number of LSB events are initiated in the base region of the model, then extended to higher levels as Re increased. In Fig. 5a, at Re= 2.81×10^5, the top-ranked state is 0000, 95.56% in terms of the percentage of the total number of the states, indicating that the flow field is dominated in a state without LSB. However, the popularity of the 0000 state gets decreased with Re increased. In Fig. 5b, at Re= 3.2×10^5, the percentage of the 0000 state drops to 62%. Therefore, Fig. 5 reveals a trend that as Re increased, LSB is developed in the base region of the cylinder. This leads to an increase in the popularity of the states coded 2048, 3840 and 3072, which all indicate the formation of LSB at z/D=1. The formation of LSB at z/D=1 at the initialization of the critical transition signifies the importance of the role of the horseshoe vortex in the base region. The interaction between the horse shoe vortex in the base region and the arch-type vortex shedding prevailing around the model deserves further study in the future. [9]

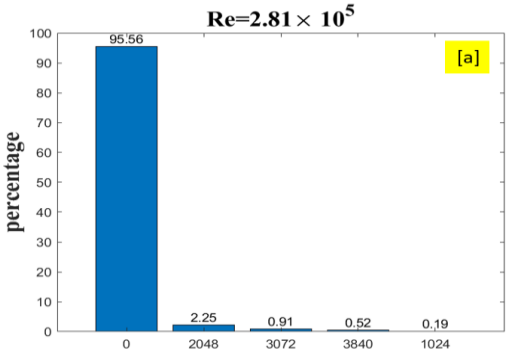

Binary [90,-90,110,-110]			Decimal	Percentage
z/D:1.0	z/D:2.0	z/D:3.5		
0000	0000	0000	0000	95.56%
1000	0000	0000	2048	2.25%
1100	0000	0000	3072	0.91%

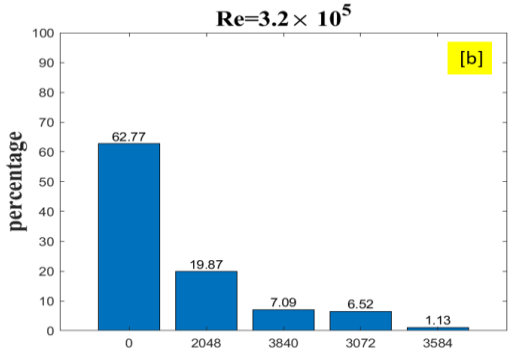

Binary [90,-90,110,-110]			Decimal	Percentage
z/D:1.0	z/D:2.0	z/D:3.5		
0000	0000	0000	0000	62.77%
1000	0000	0000	2048	19.87%
1111	0000	0000	3840	7.09%

Fig. 5 The binary statistics at pre-critical Re: (a) 2.81x10^5 and (b) 3.2x10^5.

At Re= 3.27×10^5, a case represents the transition from the pre-critical to single-sided LSB regimes, Figs. 6a and 6b indicate that the state coded 3840 is the top ranked, that LSBs are formed on both sides of the cylinder at z/D=1, and are extended over θ=θ= ±90º and ±110º, but no LSB at z/D=2 and 3.5. The trailing-behind states coded 3850, 3020, and 4010 manifest noticeable recurrences that at z/D= 3.5, LSB is formed on the positive θ side. The state 3850 indicates that no LSB is formed at z/D=2. With a close examination on the C_p traces in Figs. 6c, d and e, a physical explanation can be given below. The tip vortices originated from the free end of the model promote the formation of LSB, therefore single-sided LSB takes place in the mid-to-upper region of the model. Meanwhile, double-sided LSBs are formed stably in the base region.

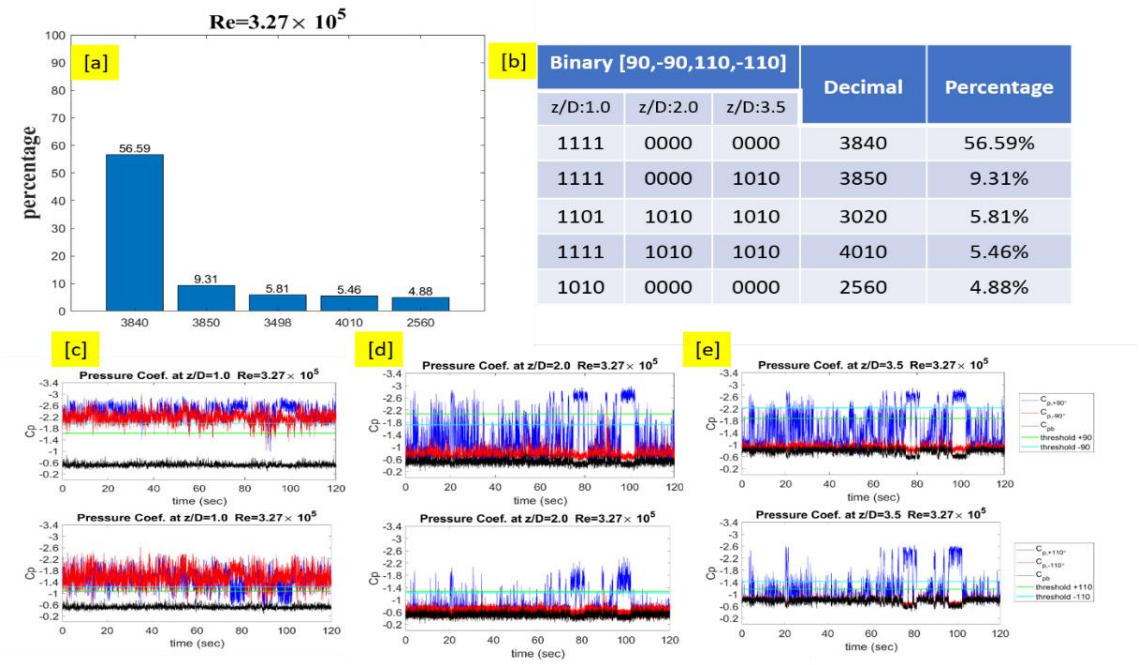

Binary [90,-90,110,-110]			Decimal	Percentage
z/D:1.0	z/D:2.0	z/D:3.5		
1111	0000	0000	3840	56.59%
1111	0000	1010	3850	9.31%
1101	1010	1010	3020	5.81%
1111	1010	1010	4010	5.46%
1010	0000	0000	2560	4.88%

Fig. 6 A case on transition from the pre-critical to one-sided LSB regimes at Re=3.27×10^5. (a) The distribution of the statistics of the top five states ranked. (b) A table listing the statistics of the top five states ranked. (c) - (e) The C_p traces at z/D= 1, 2 and 3.5.

Fig. 7 presents the results on a case in the one-sided LSB regime at Re= 3.4×10^5. In Fig. 7a, the percentages of the leading states coded 3498, 4010, and 3840 are rather comparable and count more than 75% in total. The difference between 3498 and 4010 lies in the C_p variations at θ=110º, z/D=1, indicating pronounced unsteadiness in the base region. On the other hand, the two states coded 4010 and 3840 suggest that flow around the mid and upper sections of the model is characterized by one-sided LSB with notable intermittency. In comparison with the case in Fig. 6 at slightly lower Re, it is clear that the time during which flow around the mid and upper sections remains with the presence of LSB is increased as Re increased. This infers that the higher the Reynolds number, the more stable the formation of LSB on the model.

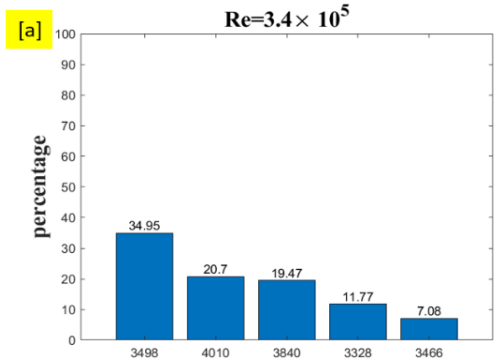

[b]

Binary [90,-90,110,-110]			Decimal	Percentage
z/D:1.0	z/D:2.0	z/D:3.5		
1101	1010	1010	3498	34.95%
1111	1010	1010	4010	20.70%
1111	0000	0000	3840	19.47%
1101	0000	0000	3328	11.77%
1101	1000	1010	3466	7.08%

Fig. 7 A case in the one-sided LSB regimes at Re=3.4×10^5. (a) The distribution of the statistics of the top five states ranked. (b) A table listing the statistics of the top five states ranked.

4. Concluding remarks

An adaptive threshold method combined with a binary ranking technique was developed in this study to quantitatively address the non-stationary characteristics of flow in the critical transition range. Since the characteristics flow in the critical transition range are pre-dominated by the unsteadiness due to formation of LSB, the present approach enables a description on the statistics of the instantaneous states regarding the formation of LSB on the model in a binary format. Subsequently, the popularity of the states can be ranked. The leading states represent the flow characteristics under the experimental condition studied. By this method, the evolution of flow through different regimes in the critical transition range can be examined in detail.

5. Acknowledgement

Funding support of National Science and Technology Council under the project number NSTC 113-2222-E-006-002 is gratefully acknowledged. Acknowledgment should also be made to the previous studies cited in this paper, from which the data are reproduced.

References

[1] A. Roshko, "Experiments on the flow past a circular cylinder at very high Reynolds number". *Journal of fluid mechanics*, Vol **10**(3), (1961), pp. 345-356.

[2] E. Achenbach and E. Heinecke, "On vortex shedding from smooth and rough cylinders in the range of Reynolds numbers 6× 103 to 5× 106". *Journal of fluid mechanics*, Vol **109**, (1981), pp. 239-251.

[3] M. Zdravkovich, "Conceptual overview of laminar and turbulent flows past smooth and rough circular cylinders". *Journal of wind engineering and industrial aerodynamics*, Vol **33**(1-2), (1990), pp. 53-62.

[4] J. Miau, H. Tsai, Y. Lin, J. Tu, C. Fang and M. Chen, "Experiment on smooth, circular cylinders in cross-flow in the critical Reynolds number regime". *Experiments in fluids*, Vol **51**, (2011), pp. 949-967.

[5] J. McClean and D. Sumner, "An experimental investigation of aspect ratio and incidence angle effects for the flow around surface-mounted finite-height square prisms". *Journal of Fluids Engineering*, Vol **136**(8), (2014), pp. 081206.

[6] S. Okamoto and Y. Sunabashiri, "Vortex shedding from a circular cylinder of finite length placed on a ground plane". Vol, (1992).

[7] R. Deshpande, V. Kanti, A. Desai and S. Mittal, "Intermittency of laminar separation bubble on a sphere during drag crisis". *Journal of Fluid Mechanics*, Vol **812**, (2017), pp. 815-840.

[8] Y.-H. Lai, J.-J. Miau, G.-T. Zhung, M.-C. Tsai and J.-C. Wu, "Characteristics of separation-bubble formation on finite circular cylinder in critical transition range". *AIAA journal*, Vol **61**(10), (2023), pp. 4468-4484.

[9] J.-J. Miau, Y.-R. Chen and Y. -H. Chen, "Evolution of flow around a finite circular cylinder in the critical transition range". The 8th International Conference on Jets, Wakes and Separated Flows, ICJWSF-2024, September 23-25, 2024, Firenze, Italy